Journal of Organometallic Chemistry 716 (2012) 120–128

Contents lists available at SciVerse ScienceDirect

Journal of Organometallic Chemistry

journal homepage: www.elsevier.com/locate/jorganchem

Bifunctional N–P ligands as building blocks for construction of multilayered metallodendrimers

Inmaculada Angurell [a,*], Esther Puig [a], Oriol Rossell [a], Miquel Seco [a,*], Pilar Gómez-Sal [b], Avelino Martín [b]

[a] Departament de Química Inorgànica, Universitat de Barcelona, Martí i Franquès 1-11, E-08028 Barcelona, Spain
[b] Departamento de Química Inorgánica, Universidad de Alcalá, E-28071 Alcalá de Henares, Spain

ARTICLE INFO

Article history:
Received 4 May 2012
Received in revised form
7 June 2012
Accepted 13 June 2012

Keywords:
Carbosilane dendrimer
Ditopic ligand
Phosphine
Metalloligands

ABSTRACT

The synthesis of 4-amino(*N*-methylendiphenylphosphino)pyridine (**1a**) and its reaction with $[PdCl_2(cod)]$, $[PtCl_2(cod)]$, $[AuCl(tht)]$, $[RuCl_2(p\text{-cymene})]_2$, $[RhCl(cod)]_2$ and $[Pd(\eta^3\text{-}2\text{-}MeC_3H_4)Cl]_2$ to give $[PdCl_2(\mathbf{1a})_2]$ (**2**), $[PtCl_2(\mathbf{1a})_2]$ (**3**), $[AuCl(\mathbf{1a})]$ (**4**), $[RuCl_2(p\text{-cymene})(\mathbf{1a})]$ (**5**), $[RhCl(cod)(\mathbf{1a})]$ (**6**) and $[Pd(\eta^3\text{-}2\text{-}MeC_3H_4)Cl(\mathbf{1a})]$ (**7**) respectively are described. The new chelate complex $[Pd(\eta^3\text{-}2\text{-}MeC_3H_4)(py\text{–}N(CH_2\text{–}PPh_2)_2)](OTf)$ (**8**) is also reported. Compounds **5** and **8** were characterized by single crystal X-ray diffraction. In all complexes prepared the metal atoms appear to be bonded through the P atom of **1a**. The metalloligands **4**, **5** and **8** have been reacted with the ruthenocarbosilanedendrimer **10** to afford new Ru–Au and Ru–Pd concentric metal layered dendrimers **11**, **12** and **13**.

1. Introduction

Dendrimer chemistry has been a subject with increasing interest in last years [1]. This development has arisen because dendrimers present unique properties, making them ideal candidates as materials in a number of nanoscale and high value added applications [2]. The unique qualities of dendrimers are attributed mainly to their controlled globular structure resulting from an internal framework in which all bonds emerge radially from a central core growing through successive generations and also to the possibility of containing a large number of functional groups which can be present in the cavities or/and at its surface. It has been shown that dendrimers are able to form complexes with a great variety of ions and metal fragments [3]. However, carbosilane dendrimers containing two or more transition metal units are scarce due to the lack of synthetic strategies [4]. Thus, new strategies for functionalization of dendrimers at the end of the branches and the use of new ligands as connectors are required in order to grow novel metalladendritic structures [5]. Bifunctional ligands containing different donor atoms (N, O, P, S) can act selectively as connectors combining soft and hard donor sites, but it should be noted that this type of ligands tend to favour the formation of chelate complexes [6]. Recently, we have described a method for the synthesis of metallodendrimers with up to four metal layers by grafting the carbosilane framework with the P–N ligands 4-py–PPh_2 and 4-py–$N(-CH_2-PPh_2)_2$ [7]. In the later case, the *trans* arrangement of the pyridine substituent and the length of the P–N chain preclude chelate formation so that the ligands act just as connectors and spacers. In this paper we present the synthesis of the P–N ligand 4-py–NH–CH_2–PPh_2, its capability to form a number of complexes with transition metal fragments and the use of these species as new building blocks to create metallodendrimers displaying concentric metal layers.

2. Results and discussion

2.1. Synthesis of 4-amino(N-methylendiphenylphosphino)pyridine (*1a*) and related transition metal complexes

The synthesis of the new phosphinoaminopyridine ligand **1a** was readily accomplished by treatment of an equimolar mixture of hydroxymethyldiphenylphosphine (obtained *in situ* from $HPPh_2$ and $(HCHO)_n$) and 4-aminopyridine in a 1:1 molar ratio at 85 °C for 24 h (Scheme 1). It is interesting to underline that the use of the same reagents in a 6:1 molar ratio leads to the ligand containing two phosphine groups (**1b**) after reaction at 120 °C for 6 days [7]. Ligand **1a** was isolated as a white solid in high yield (82%) and could routinely be prepared in gram quantities. The molecular ion peak

* Corresponding authors.
E-mail addresses: inmaculada.angurell@qi.ub.es (I. Angurell), miquel.seco@qi.ub.es (M. Seco).

0022-328X/$ – see front matter © 2012 Elsevier B.V. All rights reserved.
http://dx.doi.org/10.1016/j.jorganchem.2012.06.010

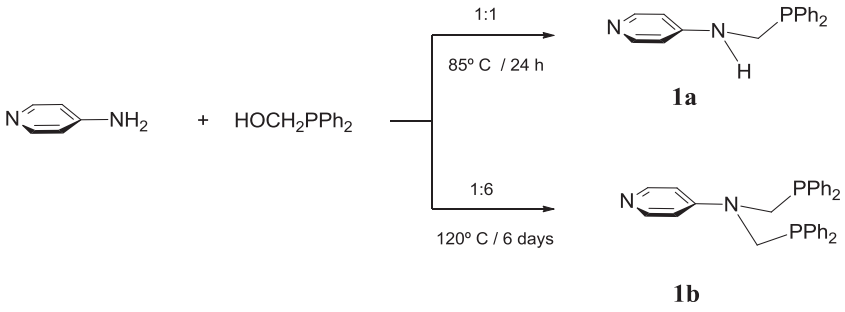

Scheme 1.

was detected at $m/z = 292.8$ $[M + H]^+$ in the (ESI-MS) spectrum, while the ^{31}P NMR spectrum in $CDCl_3$ showed a single resonance at $\delta = -18.9$ ppm. The signal at $\delta = 4.15$ ppm (N*H*) in the ^1H NMR spectrum and the IR band at 1599 cm^{-1} that is assigned to ν(C═N) stretching are other characteristic spectroscopic data for **1a**.

Given the presence of two coordination centres in **1a**, we became interested in knowing if the metal coordination occurs selectively and, in this case, which is the donor atom (N or P) responsible for the complexation. We made to react the ditopic ligand **1a** with $[PdCl_2(cod)]$ (cod = 1,5-cyclooctadiene), $[PtCl_2(cod)]$, [AuCl(tht)] (tht = tetrahydrothiophene), and with the dimeric species $[RuCl_2(p\text{-cymene})]_2$, $[RhCl(cod)]_2$ and $[Pd(\eta^3\text{-}2\text{-}MeC_3H_4)Cl]_2$ in CH_2Cl_2. In all cases metallation took place very quickly and the final mononuclear complexes **2**–**7** (Scheme 2) were isolated in good yields and fully characterized spectroscopically. The ν(C═N) stretching for **4**–**7** did not change significantly from that of the free ligand, thus indicating selective coordination through the phosphorous atoms in all cases. This is confirmed by the large shift of the signals to low fields in their ^{31}P NMR spectra (Experimental section).

For **2** and **3**, the ν(C═N) was shifted up to 1600 cm^{-1}. This fact and the insolubility of these complexes in common solvents suggest an intermolecular interaction between the *N*-pyridinic atom and the metal centre. As a result, a polymeric structure is formed. On the other hand, the *J*(P–Pt) values observed for **3** in DMSO of 1845 Hz in their ^{31}P NMR spectrum indicate a *cis* arrangement for this molecule. The protonation of the pyridine group in **2** and **3** with hydrogen chloride in CH_2Cl_2 solubilizes the complexes through formation of the corresponding cationic species $[\mathbf{2}–H]^+$ and $[\mathbf{3}–H]^+$.

The gold complex [AuCl(tht)] reacts cleanly with **1a** to give **4a** as a white solid in 96% yield. Likewise **4a** reacts with AgOTf in CH_2Cl_2 to give the compound [Au(OTf)(*P*-**1a**)] (**4b**), which can be also obtained by substitution of the PPh_3 by **1a** in [Au(OTf)(PPh_3)]. This indicates a more basic character of the *P*-**1a** than that of the PPh_3. The dimer $[RuCl_2(p\text{-cymene})]_2$ reacts with 2 equiv of the ligand **1a** to give complex **5**. The ^{31}P resonance at 20.7 ppm confirms that the coordination is *via* P atom. On the other hand, the ESI-MS spectrum in CH_3CN:H_2O shows a peak due to the $[M + H]^+$ species. Single crystals of this complex suitable for X-ray diffraction studies were obtained by slow diffusion of hexane into a dichloromethane solution of **5**. The molecular structure is shown in Fig. 1 and selected bond lengths and angles are reported in Table 1.

The X-ray analysis of complex **5** showed that the molecule displays a pseudo-octahedral geometry at Ru centre comprising one η^6-*p*-cymene, one phosphorous and two chloride atoms as ligands completing the metal coordination sphere. The moiety presents the usual three-legged piano stool arrangement with an Ru–P distance of 2.3647(11) Å, similarly to that observed in $[RuCl_2(p\text{-cymene})\{o\text{-}$

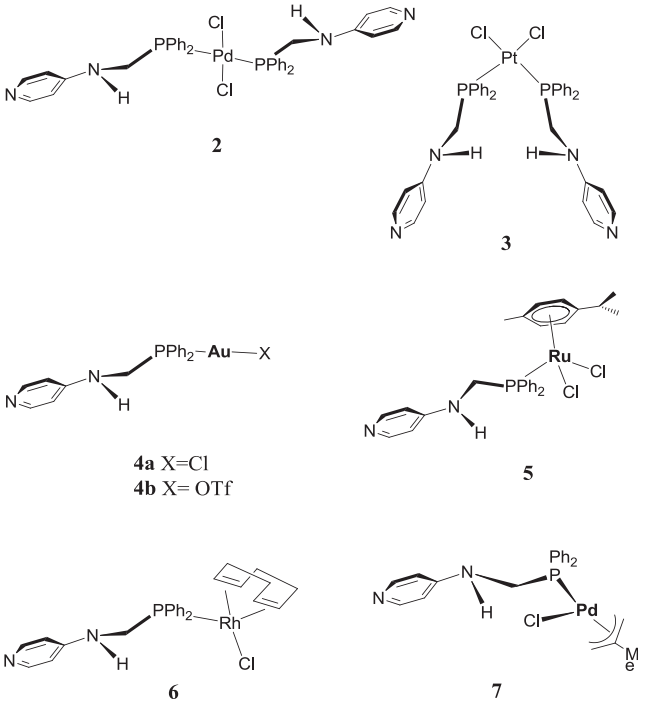

Scheme 2.

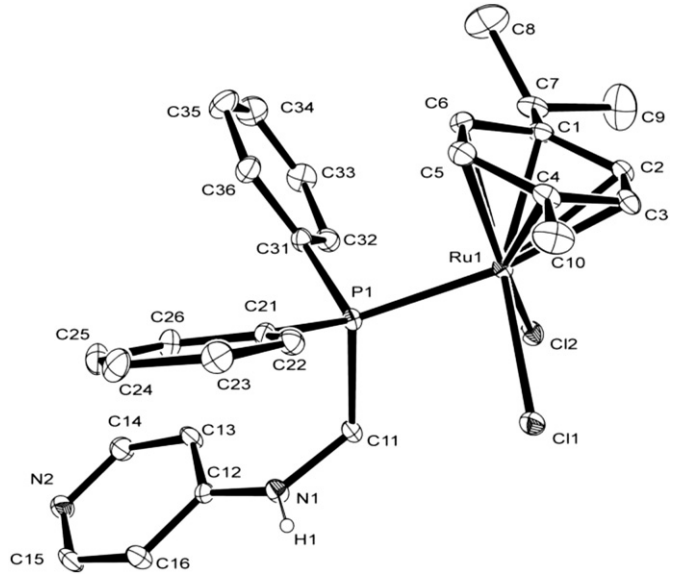

Fig. 1. Molecular structure of **5** with an atomic numbering scheme. Hydrogen atoms have been removed for clarity.

Table 1
Selected bond lengths (Å) and angles (deg) for **5**.

Ru(1)–Cl(1)	2.4248(11)
Ru(1)–Cl(2)	2.4236(11)
Ru(1)–P(1)	2.3647(11)
Ru(1)–C(1)	2.224(4)
Ru(1)–C(2)	2.233(4)
Ru(1)–C(3)	2.248(4)
Ru(1)–C(4)	2.229(4)
Ru(1)–C(5)	2.183(4)
Ru(1)–C(6)	2.178(4)
Ru(1)–Ct	1.705
P(1)–C(11)	1.889(4)
P(1)–C(21)	1.812(4)
P(1)–C(31)	1.830(4)
N(1)–C(12)	1.364(5)
N(1)–C(11)	1.441(5)
N(2)–C(14)	1.329(5)
N(2)–C(15)	1.344(5)
C(1)–C(6)	1.417(6)
C(1)–C(2)	1.434(6)
C(1)–C(7)	1.545(6)
C(2)–C(3)	1.383(6)
C(3)–C(4)	1.421(6)
C(4)–C(5)	1.401(6)
C(5)–C(6)	1.434(6)
P(1)–Ru(1)–Cl(2)	83.16(4)
P(1)–Ru(1)–Cl(1)	86.98(4)
Cl(2)–Ru(1)–Cl(1)	87.98(4)
Cl(1)-Ru(1)-Ct	126.2
Cl(2)-Ru(1)-Ct	126.7
Cl(2)–Ru(1)–Cl(1)	131.0
C(21)–P(1)–Ru(1)	118.38(14)
C(31)–P(1)–Ru(1)	109.22(13)
C(11)–P(1)–Ru(1)	113.10(14)
C(21)–P(1)–C(31)	104.53(19)
C(21)–P(1)–C(11)	102.82(19)
C(31)–P(1)–C(11)	108.0(2)
N(1)–C(11)–P(1)	118.2(3)
C(14)–N(2)–C(15)	113.4(4)
C(12)–N(1)–C(11)	126.1(4)
C(11)–N(1)–H(1)	109.2
C(12)–N(1)–C(11)	124.5

Ct is the centroid of C(1),C(2),C(3),C(4),C(5),C(6).

$Ph_2PCH_2NHC_6H_4(CH_2OH)$}] of 2.351 Å [8] or in [$RuCl_2$(*p*-cymene)(*o*-$PPh_2Py)_3$] of 2.364 Å [9]. Both Ru–Cl distances are very similar in contrast to the Ru–C ones, which range from 2.184(4) to 2.248(4) Å due to the *trans* influence of the phosphine ligand on the C(2) and C(3) atoms of the ring. This and steric factors provoke that the arene substituents adopt an alternate conformation respect to the other ligands bonded to the metal. The angle Cl–Ru–Cl of 87.98(4) Å is comparable to that found in [$RuCl_2$(*p*-cymene){*o*-$Ph_2PCH_2NHC_6H_4(CH_2OH)$}] (88.12°), and in other complexes with bulky phosphines [10]. It is interesting to note the planarity around the *N*-amine atom. The quality of the crystal allowed the localization of the amine proton H(1) and the sum of the three angles around N(1), which is 359.4°, that implies an almost perfect planarity. On the other hand the N(1)–C(12) distance of 1.364(4) Å is closer to an N–C double bond. These data indicate that the electronic lone pair of N(1) is delocalized to the aromatic ring through C(12) atom and, consequently, it has very low coordinative capacity as have been observed experimentally. An interesting feature of this structure is that the packing of the molecules is governed mainly by hydrogen bondings. Each molecule establishes two hydrogen bonds through the amino group as the proton donor and the pyridinic ring nitrogen atom as the proton acceptor with an N(1)–N(2) distance of 3.085(7) Å. The aminopyridinic system is planar, and the hydrogen bonds lies in this plane producing a lineal planar system chain, with the rest of the molecules located in alternated positions with respect to this plane (Fig. 2).

Square planar complex **6** was obtained by the reaction of the rhodium dimer $[RhCl(cod)]_2$ with **1a**. Its ^{31}P NMR spectrum showed a signal at $\delta = 23.1$ ppm with a J(P–Rh) value of 153 Hz. Both ^{1}H and ^{13}C NMR spectra revealed two signals due to the CH=CH cyclooctadiene group indicating two non-equivalent coordination metal sites due to the different trans influence of **1a** and Cl ligands.

When $[Pd(\eta^3\text{-}2\text{-}MeC_3H_4)Cl]_2$ was treated with 2 equiv of **1a** in CH_2Cl_2 the ^{31}P NMR of the solution showed that the phosphorous resonance shifted to $\delta = 18.1$ ppm. Addition of hexane precipitated the pale yellow complex **7**. Like in the case of **2** and **3**, the ν(C=N) is shifted up to 1608 cm^{-1} suggesting an intermolecular interaction between the *N*-pyridinic atom and the palladium metal centre.

Since no suitable crystals of **7** could be grown, we tried to synthesize and obtain single crystals of the analogous Pd complex with the ligand **1b** in an attempt to determine unambiguously its structure. Thus, the chelate complex $[Pd(\eta^3\text{-}2\text{-}MeC_3H_4)(py{-}N(CH_2{-}PPh_2)_2)](OTf)$ (**8**) was obtained by reacting **1b** with 1 equiv of $[Pd(\eta^3\text{-}2\text{-}MeC_3H_4)(cod)](OTf)$ in CH_2Cl_2 at room temperature [7]. The ^{31}P NMR signal of the solution reaction shifts from −27.1 (free **1b**) to 5.0 ppm. After concentration and treatment with diethylether, a light pink solid was obtained. This compound shows a band at 1586 cm^{-1} in its IR spectrum, which indicates that the pyridine group is not coordinated to the metal.

Suitable crystals for X-ray diffraction study were obtained by slow diffusion of hexane into a CH_2Cl_2 solution of **8**. A view of the molecule appears in Fig. 3, and selected bond lengths and angles are given in Table 2. One of the most relevant structural feature is the presence of a six-membered PdP_2C_2N ring with an almost planar trigonal coordination around the aminic nitrogen N(1). The bond length of C(3)–N(1) 1.397(9) Å is notably shorter than that of C(1)–N(1) 1.481 Å or C(2)–N(1) 1.478 Å and of the same value observed in the ruthenium complex **5** described above. Therefore, there is a high degree of delocalization of the N(1) lone pair between the dimethylene-amino group and the pyridine ring. Similar effect has been observed in complexes containing the 4-(*N*,*N*-dimethylamino)pyridine ligand

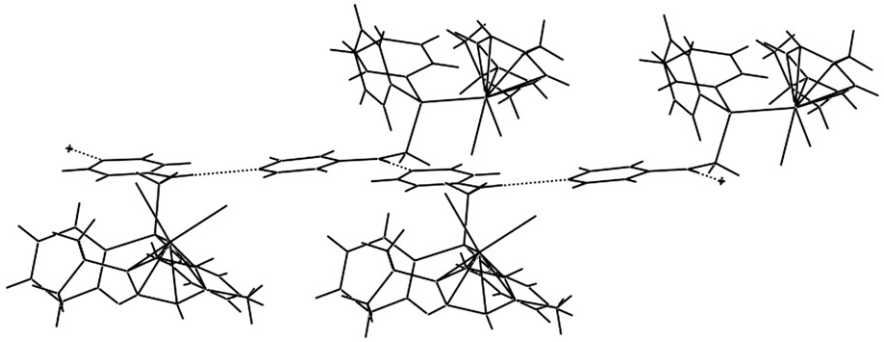

Fig. 2. The molecules of **5** are connected *via* hydrogen bonding to form strings where all aminopyridine moieties are coplanar.

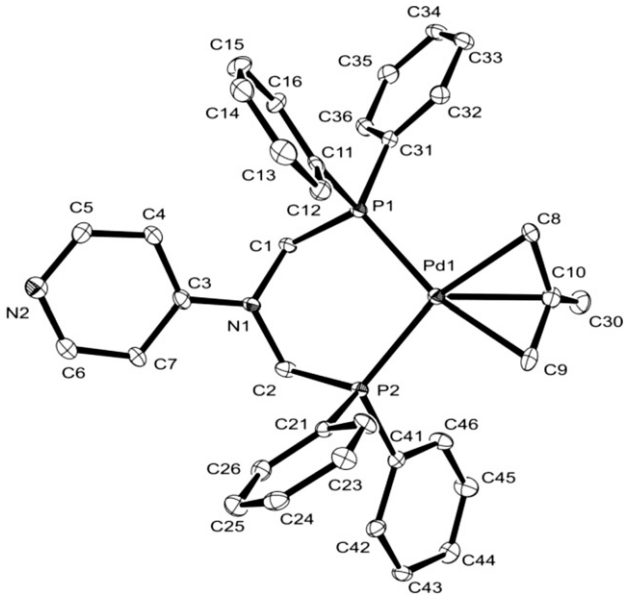

Fig. 3. Crystal structure of the cationic moiety of **8** with a numbering scheme.

[11]. The delocalization of its lone pair on the pyridinic ring makes all N-surrounding atoms of the $(CH_2)_2$–N–py fragment in the same plane indicating that free rotation around the C(3)–N(1) bond is not permitted. The presence of a trigonal planar nitrogen atom in the ring makes **8** to adopt a chair conformation with the palladium atom displaying a slightly distorted four-coordinate square planar coordination. Thus, the geometry around the palladium atom is similar to that observed in other Pd–allyl complexes. In particular, the allyl group is almost symmetrically bound [(Pd–C9) 2.180 (7) Å; (Pd–C8) 2.196(7) Å] and forms a dihedral angle of 113.1(5)° with the plane defined by the Pd atom and the phosphorous atoms, close to the typical value found in η^3-allyl Pd and Pt complexes [12]. On the other hand the Pd–P and P–C distances are in the expected range observed in other π-allylic Pd(II) complexes containing phosphines and the 2-Me–allyl fragment [13].

Table 2
Selected bond lengths (Å) and angles (°) for the solid-sate structure of the cationic moiety of **8**.

Pd(1)–C(8)	2.196(7)
Pd(1)–C(9)	2.180(7)
Pd(1)–C(10)	2.215(8)
Pd(1)–P(1)	2.3125(18)
Pd(1)–P(2)	2.3335(19)
P(1)–C(11)	1.829(7)
P(1)–C(1)	1.873(7)
P(1)–C(31)	1.846(7)
P(2)–C(2)	1.852(7)
P(2)–C(21)	1.832(7)
P(2)–C(41)	1.842(7)
C(1)–N(1)	1.482(8)
C(2)–N(1)	1.478(9)
C(3)–N(1)	1.397(9)
N(2)–C(5)	1.364(10)
N(2)–C(6)	1.341(10)
P(1)–Pd(1)–P(2)	97.71(7)
C(9)–Pd(1)–P(1)	165.9(2)
C(8)–Pd(1)–P(1)	99.4(2)
C(10)–Pd(1)–P(1)	129.9(2)
C(9)–Pd(1)–P(2)	96.3(2)
C(8)–Pd(1)–P(2)	162.7(2)
C(10)–Pd(1)–P(2)	128.3(2)
C(9)–Pd(1)–C(8)	66.5(3)
C(9)–Pd(1)–C(10)	37.6(3)
C(8)–Pd(1)–C(10)	37.5(3)
C(1)–P(1)–Pd(1)	110.4(2)
C(2)–P(2)–Pd(1)	113.5(2)
N(1)–C(1)–P(1)	115.2(4)
N(1)–C(2)–P(2)	113.6(5)
C(1)–N(1)–C(2)	113.1(6)
C(3)–N(1)–C(1)	120.2(5)
C(3)–N(1)–C(2)	124.1(6)
C(6)–N(2)–C(5)	113.9(7)

2.2. Synthesis of polymetallodendrimers

As starting material for the synthesis of new metallodendrimers we employed the carbosilane dendrimer **9**, functionalized with diphenylphosphine groups at surface described previously (Scheme 3) [14].

The methodology for the construction of dendrimers containing several metal layers involved three steps: i) grafting of organometallic ruthenium moieties on the surface of a phosphine ended carbosilane dendrimer by reaction with $[RuCl_2(p\text{-cymene})]_2$ to give the metallodendrimer **9** and chloride substitution by OTf ligands to obtain **10** (Scheme 3); ii) displacement of one OTf ligand by N-coordination of **1a** and iii) incorporation of a new metal fragment taking advantage of the presence of free phosphine at the periphery. Surprisingly, the solution resulting from step ii) showed broad signals indicating the existence of dynamic processes in solution. The main signals appeared at 29.5 and −1.0 ppm, which are assigned to the $-PPh_2$ group bonded to the Ru atom and to the free $-PPh_2$ group of **1a**, respectively. Besides, two minor signals appeared as doublets at 29.0 and 21.4 ppm. After several hours at room temperature, the ^{31}P NMR spectrum showed that the latter resonances increased until to reach equilibrium. This equilibrium between the species resulting from the coordination through the N or P donor atoms underlines the lack of selectivity in the process, and finally the thermodynamically more stable *P*-**1a** form predominates (Scheme 4).

To overcome this drawback, we decided to block the phosphine centre using **4a** as metalloligand instead **1a**. Thus, a CH_2Cl_2 solution of the ruthenodendrimer **10** was reacted with **4a** in a 1:4 molar ratio. The yellow colour suddenly changed to deep orange and a white suspension was formed. After filtration, the IR spectrum of the white solid revealed the presence of the triflate anion, and the bands at 1613 ($\nu_{(C{=}N)}$) and 1102 cm^{-1} (PPh_2 group) suggest that the ligand **1a** was coordinated to the metal by both N and P ended donor atoms. The ESI-MS spectrum showed an intense peak at 2404.8 that can be assigned to the $[4\{Au(OTf)(\mathbf{1a})\} - OTf]^+$ unit and other minor peaks corresponding to the lost of $\{Au(OTf)(\mathbf{1a})\}$ fragments. These results suggest that the insoluble solid probably is the result of the association of four $\{Au(\mathbf{1a})\}$ units to give the tetrameric species $[\{Au(\mathbf{1a})\}_4](OTf)_4$ (Scheme 5).

On the other hand, the ^{31}P NMR spectrum of the solution evidenced only a signal at 22.2 ppm, not far from the one that appears in the spectrum of **10**. We suspected that the resulting compound was the chiral ruthenium compound having four different ligands, **1a**, Cl, OTf, and *p*-cymene. The ^{31}P NMR resonance at 22.6 ppm of

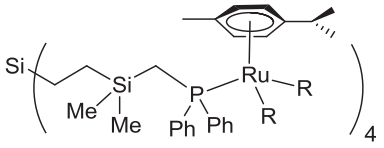

9 R = Cl
10 R = OTf

Scheme 3. Metallodendrimers **9** and **10**.

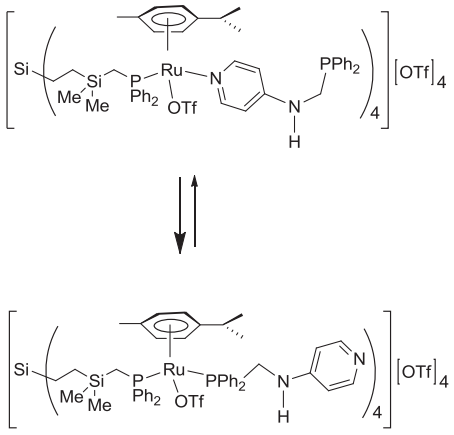

Scheme 4.

the product resulting after treatment of the chiral ruthenium compound with AgOTf corroborated our assumption. In conclusion, we postulate that the reaction of **10** with **4a** takes place through three paths: coordination of the metalloligand, migration of the chloride from gold to the ruthenium atom, followed finally by the decoordination of the ligands [15] (Scheme 5).

With these results in mind, we reasoned that dendrimers containing both metal atoms only could be stabilized if the chloride migration is prevented. Clearly, the use of metalloligand **4b** could favour this goal. Indeed, reaction of **4b** with dendrimer **10** in a 4:1 molar ratio in CH_2Cl_2 at room temperature permitted to observe only two signals in its $^{31}P\{^1H\}$ NMR spectrum at 29.6 ppm (Ru–*P*Ph_2) and 35.6 ppm (Au–*P*Ph_2). After work up the dendrimer **11** was isolated as an ochre-yellow solid in high yield. Compound **11** was fully characterized by IR, ^1H and ^{13}C NMR spectroscopy and elemental analysis (Experimental section).

Attempts to extend this methodology for the synthesis of other bi-metallodendrimers were not successful: the reaction of **10** with the metalloligands **5**, **6** and **7** gave complicated mixture of different species in solution that were not investigated. Probably the steric crowding of the resulting species due to the higher volume of the latter metalloligands is responsible for this behaviour.

These results made us to turn our attention to ligand **1b** and, in particular to [4-py–N{CH_2–PPh_2AuOTf}$_2$] that was chosen as metalloligand to react with **10**. The reaction was performed in CH_2Cl_2 at room temperature and the dendrimer **12** was isolated as an orange-brown solid in high yield (Scheme 6). The $^{31}P\{^1H\}$ spectrum of this compound showed signals at $\delta = 25.8$ (Ru–*P*Ph_2) and $\delta = 19.4$ ppm (Au–*P*Ph_2) and its $^{13}C\{^1H\}$ NMR spectrum a resonance at 152.5 ppm assigned to the C_α of the pyridinic ring. However, solutions of the new bimetallodendrimer showed progressive degradation in hours. The lower stability of **12** in comparison to that of **11** should be mainly attributed to the higher steric hindrance expected for the first. Then, we reasoned that the use of a chelating metalloligand such as **8**, where the arms are close one to another would favour the coordination and stabilization of the final product. Thereby, when a solution of **8** was treated with the dendrimer **10** a change of colour in the solution was immediately observed. After 15 min the $^{31}P\{^1H\}$ spectrum of the solution showed the shifting of the signal (Ru*P*) at 29.8 ppm confirming the coordination of **8** to the ruthenium atom. After work up dendrimer **13** was obtained as a deep yellow solid stable in solution (Scheme 7).

Although the ESI-MS spectrum showed great fragmentation, both the NMR and IR data support the nature of the Ru/Pd dendrimer (Experimental section).

3. Conclusions

The new aminophosphine ligand **1a** was synthesized from 4-aminopyridine and hydroxymethyldiphenylphosphine in high yield. Metallocomplexes of Au, Pd, Pt, Ru, Rh are easily formed by direct reaction between ligand **1a** and the corresponding transition metal compounds. The gold complex **4b** has permitted to construct a bimetallic carbosilane dendrimer containing two concentric metal layers of Ru and Au. In contrast, Ru, Rh and Pd complexes gave untreatable mixtures. However, the use of a chelate Pd complex with

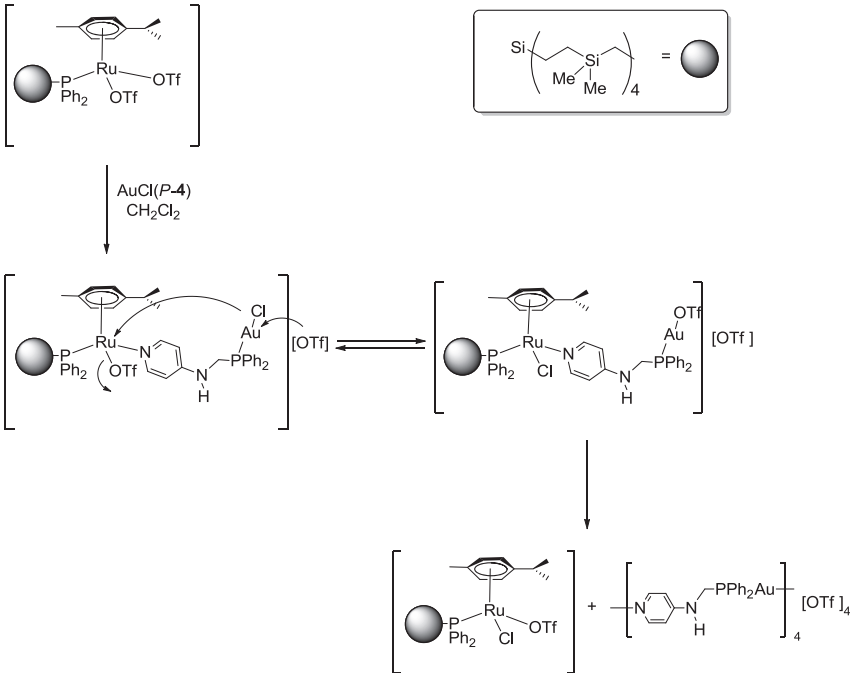

Scheme 5.

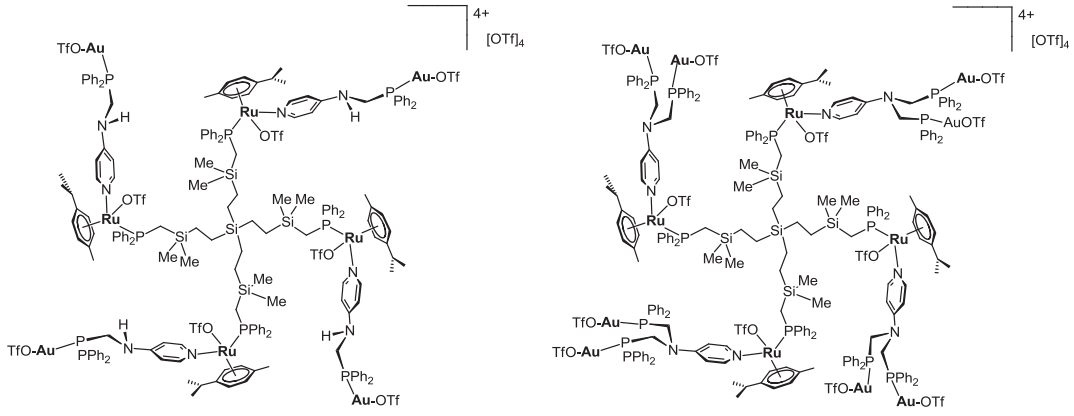

11 12

Scheme 6.

ligand **1b** (4-amino[*N*,*N*′-bis(methylenediphenylphosphino)pyridine]), that can be obtained by modification of the method described for **1a**, has allowed to form a new very stable dendrimer containing two metal layers, one of Ru and the other of Pd.

4. Experimental section

4.1. General considerations

All manipulations were performed under an atmosphere of dry nitrogen using standard Schlenk techniques. All solvents were distilled from appropriate drying agents prior to use. Gold complexes were synthesized light protected to avoid metal reduction. ^{1}H, $^{13}C\{^{1}H\}$ and $^{31}P\{^{1}H\}$ NMRspectra were recorded on Bruker 250 and Varian Mercury 400 spectrometers. Chemical shifts are reported in parts per million relative to external standards ($SiMe_4$ for ^{1}H and ^{13}C, 85% H_3PO_4 for ^{31}P) and coupling constants are given in hertz. Infrared spectra were recorded with an FTIR 520 Nicolet spectrophotometer (KBr pellets). Elemental analyses of C, H and N were carried out at the Serveis Científico-Tècnics in Barcelona. ESI-MS spectra were recorded with an Agilent LC/MSD-TOF spectrometer. The starting materials, [Pd(η^3-2-MeC_3H_4)(cod)](OTf) [16], [AuCl(tht)] [17], [$RuCl_2$(*p*-cymene)]$_2$ [18], 4-pyridyldiphenylphosphine [19], [RhCl(cod)]$_2$ [20], [$PdCl_2$(cod)] [21], [$PtCl_2$(cod)] [22], and dendrimer **9** [14,23] were prepared following published procedures. Other reagents were purchased from commercial suppliers. It is noticeable that synthesis for compound **1a** in benzene solution by a typical Mannich reaction in 71% yield has been described in the course of time of this work [24].

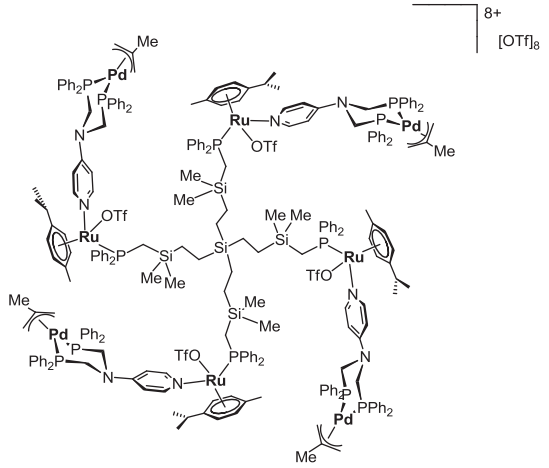

13

Scheme 7.

4.2. X-ray structure determination of compounds *5* and *8*

Suitable monocrystals of compounds **5** and **8** were obtained by slow diffusion of hexane into a CH_2Cl_2 solution of them. A summary of crystal data, data collection, and refinement parameters for the structural analysis is given in Table 3. Crystals were glued to a glass fibre using an inert polyfluorinated oil and mounted in the low temperature N_2 stream (200 K), in a Bruker-Nonius Kappa-CCD

Table 3
Summary of crystal data and structure refinement parameters for **5** and **8**.

Compound	**5**	**8**
Empirical formula	$C_{28}H_{31}Cl_2N_2PRu$	$C_{36}H_{35}F_3N_2O_3P_2PdS$
Formula weight	598.49	801.06
Crystal system	Monoclinic	Monoclinic
Space group	$P21/c$	$P2_1/n$
a/Å	13.4476(19)	9.147(5)
b/Å	12.5288(5)	24.545(5)
c/Å	15.777(2)	15.350(5)
β°	96.270(13)	96.060(5)
V/Å^3	2642.2(5)	3427(2)
Z	4	4
D_c/g cm^{-3}	1.504	1.553
Absorption coeff./mm^{-1}	0.876	0.752
F(000)	1224	1632
Crystal size, mm	0.35 × 0.3 × 0.2	0.6 × 0.3 × 0.2
Θ Range for data collection	3.05–26.52°	3.14–27.51°
Limiting indices	$-16 \le h \le 16$ $-15 \le k \le 15$ $-19 \le l \le 19$	$-11 \le h \le 11$ $-31 \le k \le 31$ $-0 \le l \le 19$
Total reflections	19,507	15,402
Unique reflections	5473	7859
R(int)	0.1335	0.1144
Completeness to q	q = 26.52 (99.8%)	q = 27.51 (99.8%)
Max. and min. transm.	0.853 and 0.728	1.204 and 0.884
Refinement method	Full-matrix least-squares on F^2	Full-matrix least-squares on F^2
Data/restraints/parameters	5473/0/319	7859/0/433
Goodness-of-fit on F^2	0.802	1.008
Final R indices [$I > 2\sigma(I)$]	R1 = 0.0400, $wR2$ = 0.0697	$R1$ = 0.0817, $wR2$ = 0.1871
R indices (all data)	$R1$ = 0.0992, $wR2$ = 0.0843	$R1$ = 0.1570, $wR2$ = 0.2184
Largest diff. peak and hole/e Å^{-3}	0.608 and −0.697	1.615 and −1.494

diffractometer with area detector equipped with an Oxford Cryostream 700 unit. Intensities were collected using graphite monochromated Mo–K_α radiation (l = 0.71073 Å). Data of compound **5** were measured with an exposure time of 10 s per frame (five sets; 237 frames; Φ/Ω scans, 2.0° scan-width), compound **8** with an exposure time of 13 s per frame (eight sets; 662 frames; Φ/Ω scans 1.3° scan-width). Raw data were corrected for Lorenz and polarization effects. Structure was solved by direct methods, completed by the subsequent difference Fourier techniques and refined by full-matrix least-squares on F^2(SHELXL-97) [25]. Anisotropic thermal parameters were used in the last cycles of refinement for the non hydrogen atoms in both structures. Absorption correction procedures, semi-empirical from equivalents, were carried out using the multiscan SORTAV program [26]. Most of the hydrogen atoms were included from geometrical calculations and refined using a riding model. The aminic Hydrogen H(1) and the methylene hydrogen atoms H(11A) and H(11B) in **8** were located in the Fourier difference map and refined isotropicaly. All the calculations were made using the WINGX system [27].

4.3. Synthesis

4.3.1. Synthesis of 4-amino-(N-methylendiphenylphosphine) pyridine (*1a*)

A mixture of *p*-formaldehyde (0.375 g, 12.5 mmol) and diphenylphosphine (2.05 cm^3, 11.9 mmol) was heated at 120 °C for 5 h to yield Ph_2PCH_2OH. The yellow oil obtained was left to reach room temperature and 4-aminopyridine (1.037 g, 10.8 mmol) was added. The reaction mixture was heated to 85 °C for 24 h and the white solid obtained was dissolved in THF and dried with anhydrous Na_2SO_4. Then, the solvent was evaporated to dryness and the resulted solid was washed with ethyl ether (2 × 50 cm^3), filtered and dried under vacuum. Compound **1a** was obtained as a white solid in 78% yield and is soluble in THF, CH_2Cl_2, MeOH and insoluble in acetone, ethyl acetate, Et_2O, toluene and hexane. ^{1}H NMR (250.13 MHz, $CDCl_3$) δ (ppm) = 3.84 (dd, 2H, $^2J_{H-P}$ = 5.5 Hz, $^3J_{H-H}$ = 4.3 Hz, C*H*$_2$P), 4.15 (br s, 1H, N*H*), 6.46 (dd, 2H, $^3J_{H-H}$ = 4.9 Hz, $^5J_{H-H}$ = 1.5 Hz, H_β), 7.36–7.48 (m, 10H, C_6H_5), 8.20 (dd, 2H, $^3J_{H-H}$ = 4.9 Hz, $^5J_{H-H}$ = 1.5 Hz, H_α). ^{13}C{^{1}H} NMR (62.90 MHz, $CDCl_3$) δ (ppm) = 42.2 (d, $^1J_{C-P}$ = 13.1 Hz, *C*H$_2$P), 107.9 (s, C_β), 128.9 (d, $^3J_{C-P}$ = 6.7 Hz, *m*-C_6H_5), 129.4 (s, *p*-C_6H_5), 132.8 (d, $^2J_{C-P}$ = 18.3 Hz, *o*-C_6H_5), 135.5 (d, ^1J(C–P) = 12.8 Hz, *ipso*-C_6H_5), 150.0 (s, C_α), 153.2 (d, $^3J_{C-P}$ = 4.8 Hz, C_γ). ^{31}P{^{1}H} NMR (101,25 MHz, $CDCl_3$) δ (ppm) = −18.9 (s, *P*Ph$_2$). IR (KBr) ν(C=N)$_{py}$ 1599 cm^{-1}. ESI-MS: (*m*/*z*) 292.8 [M + H]$^+$, 202.2 [M − pyNH]$^+$, 187.1 [M − pyNHCH$_2$]$^+$, 107.2 [M − PPh$_2$]$^+$. Elem. anal. for $C_{18}H_{17}N_2P$ (290.32): calcd (%) C, 74.46; H, 5.20. Found: C, 73.85; H, 5.75.

4.3.2. Synthesis of *2*

To a solution of **1a** (0.237 g, 0.81 mmol) in 20 cm^3 of CH_2Cl_2 complex [$PdCl_2$(cod)] (0.112 g, 0.40 mmol) was added and the mixture was stirred overnight. Then, the solid was filtered off and washed with CH_2Cl_2 (3 × 5 cm^3) and dried under reduced pressure. A second fraction of compound is obtained by concentration of the solution to dryness and washed the residue with CH_2Cl_2 (3 × 5 cm^3). Finally the solid was dried under vacuum to obtain **2** as an orange solid in 92% yield. ^{1}H NMR (300.00 MHz, DMSO-d_6) δ (ppm) = 3.81 (m, 4H, C*H*$_2$P), 4.08 (br s, 2H, N*H*), 6.56 (d, 4H, $^3J_{H-H}$ = 7.2 Hz, H_β), 7.32–7.91 (m, 20H, C_6H_5), 8.00 (d, 4H, $^3J_{H-H}$ = 5.2 Hz, H_α). ^{31}P{^{1}H} NMR (101.25 MHz, $CDCl_3$) δ (ppm) = 26.0 (s, *P*Ph$_2$). IR (KBr) ν(C=N)$_{py}$ 1615 cm^{-1}. ESI-MS: (*m*/*z*) 763.0 [M + H]$^+$, 727.0 [M − Cl]$^+$, 362.9 [M − 2Cl + 2H$_2$O]$^{2+}$, 293.1 [**1** + H]$^+$. Elem. anal. for $C_{36}H_{34}Cl_2N_4P_2Pd$ (761.93): calcd (%) C, 56.75; H, 4.50. Found: C, 56.51; H, 4.35.

4.3.3. Synthesis of *3*

To a solution of **1a** (0.309 g, 1.06 mmol) in 25 cm^3 of CH_2Cl_2 complex [$PtCl_2$(cod)] (0.132 g, 0.35 mmol) was added and the mixture was stirred under reflux overnight. Then, the suspension was filtered and the solid was washed with $CHCl_3$ (3 × 5 cm^3) and dried under a vacuum. Compound **3** was obtained as a pale yellow solid in 89% yield. ^{31}P{^{1}H} NMR (101.25 MHz, DMSO-d_6) δ (ppm) = 5.8 (s, ^1J(P–Pt) = 1845 Hz, PPh$_2$). IR (KBr) ν(C=N)$_{py}$ 1620 cm^{-1}. ESI-MS: (*m*/*z*) 815.1 [M − Cl]$^+$. Elem. anal. for $C_{36}H_{34}Cl_2N_4P_2Pt$ (850.61): calcd (%) C, 50.83; H, 4.03. Found: C, 50.31; H, 3.85.

4.3.4. Synthesis of *4a*

Ligand **1a** (0.176 g, 0.60 mmol) was solved in 25 cm^3 of CH_2Cl_2 and [AuCl(tht)] (0.183 g, 0.57 mmol) was added. The mixture was stirred at room temperature, light protected, for 4 h. The resulted solution was concentrated to 10 cm^3 and 20 cm^3 of hexane was added. The mixture was filtered and the solid was washed with hexane (3 × 5 cm^3) and dried under vaccum. Compound **4a** was obtained as a white solid in 96% yield. ^{1}H NMR (250.13 MHz, $CDCl_3$) δ (ppm) = 4.28 (br s, 2H, C*H*$_2$P), 5.06 (br s, 1H, N*H*), 6.49 (d, 2H, $^3J_{H-H}$ = 4.6 Hz, H_β); 7.49–7.74 (m, 10H, C_6H_5), 8.13 (d, 2H, $^3J_{H-H}$ = 4.2 Hz, H_α). ^{13}C{^{1}H} NMR (62.90 MHz, $CDCl_3$) δ (ppm) = 42.9 (d, $^1J_{C-P}$ = 44.3 Hz, *C*H$_2$P), 108.6 (s, C_β), 129.8 (d, $^3J_{C-P}$ = 8.1 Hz, *m*-C_6H_5), 132.9 (s, *p*-C_6H_5), 133.8 (d, $^2J_{C-P}$ = 9.1 Hz, *o*-C_6H_5), 149.2 (s, C_α), 153.0 (br s, C_γ). ^{31}P{^{1}H} NMR (101.25 MHz, $CDCl_3$) δ (ppm) = 25.5 (s, *P*Ph$_2$). IR (KBr) ν(C=N)$_{py}$ 1596 cm^{-1}. ESI-MS: (*m*/*z*) 781 [2M − 2Cl]$^+$, 525 [M + H]$^+$, 507 [M − Cl + H$_2$O]$^+$, 489 [M − Cl]$^+$, 293 [M − AuCl + H]$^+$. Elem. anal. for $C_{18}H_{17}AuClN_2P$ (524.74): calcd (%) C, 41.20; H, 3.27. Found: C, 40.91; H, 3.30.

4.3.5. Synthesis of *4b*

To a solution of [AuCl(PPh$_3$)] (0.069 g, 0.14 mmol) in 5 cm^3 of CH_2Cl_2, AgOTf (0.038 g, 0.15 mmol) was added and the mixture was stirred at room temperature for 30 min, light protected. The solution was filtered off (Celite), concentrated to 5 cm^3, and was slowly added to 0.041 g (0.14 mmol) of ligand **1a** solved in 5 cm^3 of CH_2Cl_2. The mixture was stirred for 1 h. The solution was concentrated to half volume and ethyl ether was added to precipitate **4b** as a white solid, which was filtered, washed with Et_2O (3 × 5 cm^3) and vacuum dried. Yield 98%. ^{1}H NMR (250.13 MHz, $CDCl_3$) δ (ppm) = 4.46 (dd, 2H, $^2J_{H-P}$ = 11.5 Hz, $^3J_{H-H}$ = 2.8 Hz, C*H*$_2$P), 6.36 (d, 2H, $^3J_{H-H}$ = 5.0 Hz, H_β), 6.57 (br s, 1H, N*H*), 7.38–7.55 (m, 10H, C_6H_5), 7.94 (d, 2H, $^3J_{H-H}$ = 5.0 Hz, H_α). ^{13}C{^{1}H} NMR (62.90 MHz, $CDCl_3$) δ (ppm) = 44.3 (d, ^1J(C–P) = 27.2 Hz, *C*H$_2$P), 108.3 (s, C_β), 129.9 (s, *m*-C_6H_5), 132.3 (s, *p*-C_6H_5), 133.5 (s, *o*-C_6H_5), 134.2 (br s, *i*-C_6H_5), 149.7 (s, C_α), 153.0 (s, C_γ). ^{31}P{^{1}H} RMN (101.25 MHz, $CDCl_3$) δ (ppm) = 34.2 (br s, *P*Ph$_2$). ^{19}F NMR (376.48 MHz, $CDCl_3$) δ (ppm) = −78.6 (s, C*F*$_3$SO$_3$). IR (KBr) ν(C=N)$_{py}$ 1599 cm^{-1}. ESI-MS: (*m*/*z*) 931.3 [M + **1** + H]$^+$, 781.3 [M − OTf + **1**]$^+$, 639.1 [M + H]$^+$, 293.2 [M − AuOTf + H]$^+$. Elem. anal. for $C_{19}H_{17}AuF_3N_2O_3PS$ (638.3): calcd (%) C, 35.75; H, 2.68. Found: C, 36.10; H, 2.76.

4.3.6. Synthesis of *5*

To a solution of **1a** (0.051 g, 0.18 mmol) in 10 cm^3 of CH_2Cl_2 complex [$RuCl_2$(*p*-cymene)]$_2$ (0.053 g, 0.09 mmol) was added and the mixture was stirred at r.t. for 1 h. Then, the solvent was evaporated to dryness, and the residue was washed with Et_2O (3 × 5 cm^3) and dried under reduced pressure. Compound **5** was obtained as an orange solid in 94% yield. ^{1}H NMR (250.13 MHz, $CDCl_3$) δ (ppm) = 0.92 (d, 6H, $^3J_{H-H}$ = 7.0 Hz, C*H*$_{3cym}$), 1.88 (s, 3H, C*H*$_{3cym}$), 2.55 (m, 1H, $^3J_{H-H}$ = 6.7 Hz, C*H*$_{cym}$), 4.48 (dd, 2H, $^2J_{H-P}$ = 6.5 Hz, $^3J_{H-H}$ = 2.1 Hz, 2H, C*H*$_2$P), 5.19–5.30 (m, 5H, C_6H_4, N*H*), 6.05 (dd, 2H, $^3J_{H-H}$ = 6.4 Hz, $^5J_{H-H}$ = 3.5 Hz, H_β), 7.40–7.44 (m, 6H, C_6H_5), 7.81–7.89 (m, 6H, C_6H_5 + H_α). ^{13}C{^{1}H} NMR (62.90 MHz,

$CDCl_3$) δ (ppm) = 17.7 (s, CH_{3cym}), 21.8 (s, CH_{3cym}), 30.4 (s, CH_{3cym}), 41.2 (d, $^1J_{C-P}$ = 29.2 Hz, CH_2P), 86.2 (d, $^2J_{C-P}$ = 5.0 Hz, C_{cym}), 90.2 (d, $^2J_{C-P}$ = 4.0 Hz, C_{cym}), 95.6 (s, C_{cym}), 107.4 (s, C_{cym}), 109.3 (s, C_{cym}), 128.9 (d, $^3J_{C-P}$ = 9.1 Hz, *m*-C_6H_5), 131.5 (br s, *p*-C_6H_5), 131.8 (d, $^3J_{C-P}$ = 42.3 Hz, *i*-C_6H_5), 133.7 (d, $^2J_{C-P}$ = 9.1 Hz, *o*-C_6H_5), 149.0 (s, C_α), 153.2 (br s, C_γ). $^{31}P\{^1H\}$ NMR (101.25 MHz, $CDCl_3$) δ (ppm) = 20.7 (s, PPh_2). IR (KBr) ν(C=N)$_{py}$ 1602 cm^{-1}. ESI-MS: (*m*/*z*) 598.9 $[M + H]^+$, 563.0 $[M - Cl]^+$, 292.9 [M − $RuCl_2$(*p*-cymene) + H]$^+$. Elem. anal. for $C_{28}H_{31}Cl_2N_2PRu$ (598.5): calcd (%) C, 56.19; H, 5.22. Found: C, 55.70; H, 5.06.

4.3.7. Synthesis of **6**

To a solution of **1a** (0.163 g, 0.56 mmol) in 25 cm^3 of CH_2Cl_2, complex $[RhCl(cod)]_2$ (0.137 g, 0.28 mmol) was added and the mixture was stirred at r.t. for 1 h. Then, the mixture was filtered through Celite and the solution was concentrated to reduced the volume to 5 cm^3, and 10 cm^3 of hexane was added to obtain **6** as a yellow solid, which was filtered off, washed with toluene (2 × 5 cm^3) and dried under reduced pressure. Yield 83%. ^1H NMR (250.13 MHz, $CDCl_3$) δ (ppm) = 2.44 (m, 8H, cod CH_2), 3.05 (br s, 2H, cod *H*C=C*H*), 4.19 (pt, 2H, $^2J_{H-P}$ = 5.2 Hz, CH_2P), 5.54 (br s, 2H, cod *H*C=C*H*), 6.45 (d, 2H, $^3J_{H-H}$ = 7.0 Hz, H_β), 6.59 (br s, 1H, N*H*), 7.12–7.67 (m, 10H, C_6H_5), 8.11 (d, 2H, $^3J_{H-H}$ = 6.9 Hz, H_α). $^{13}C\{^1H\}$ NMR (62.90 MHz, $CDCl_3$) δ (ppm) = 28.7 (s, cod CH_2), 33.1 (s, cod CH_2), 42.8 (d, $^1J_{C-P}$ = 30.2 Hz, CH_2P), 71.7 (s, cod HC=CH), 107.3 (br s, cod HC=CH), 108.6 (s, C_β), 128.9 (d, $^3J_{C-P}$ = 10.1 Hz, *m*-C_6H_5), 130.4 (d, $^1J_{C-P}$ = 40.2 Hz, *i*-C_6H_5), 131.1 (s, *p*-C_6H_5), 133.7 (d, $^2J_{C-P}$ = 11.1 Hz, *o*-C_6H_5), 150.4 (s, C_α), 153.8 (d, $^3J_{C-P}$ = 7.0 Hz, C_γ). $^{31}P\{^1H\}$ NMR (101.25 MHz, $CDCl_3$) δ (ppm) = 23.1 (d, $^1J_{P-Rh}$ = 153.1 Hz, PPh_2). IR (KBr) ν(C=N)$_{py}$ 1616 cm^{-1}. ESI-MS: (*m*/*z*) 539 $[M + H]^+$, 503 $[M - Cl]^+$. Elem. anal. for $C_{26}H_{29}ClN_2PRh$ (538.8): calcd (%) C, 57.95; H, 5.42. Found: C, 55.70; H, 5.16.

4.3.8. Synthesis of **7**

To a solution of **1a** (0.190 g, 0.65 mmol) in 20 cm^3 of CH_2Cl_2, complex $[Pd(\eta^3\text{-}2\text{-}MeC_3H_4)Cl]_2$ (0.128 g, 0.32 mmol) was added and the pale yellow solution was stirred at r.t. for 45 min. Then, the solution was concentrated to half volume and hexane was added to precipitate **7** as a yellow solid, which was filtered and recrystallized in CH_2Cl_2/Et_2O and vacuum dried. Yield 72%. ^1H NMR (250.13 MHz, $CDCl_3$) δ (ppm) = 2.10 (br s, CH_{3allyl}), 3.58–2.57 (br s, CH_{2allyl}), 4.27 (br s, CH_2P), 4.57 (s, N*H*), 6.30 (d, H_β), 7.40–7.70 (m, C_6H_4), 8.04 (s, H_α). $^{13}C\{^1H\}$ NMR (100.61 MHz, CD_2Cl_2) δ (ppm) = 25.8 (s, CH_{3allyl}), 42.6 (br s, CH_2P), 58.2 (br s, CH_{2allyl}), 76.2 (br s, CH_{2allyl}), 110.4 (s, C_β), 128.7–140.5 (m, C_6H_5), 141.8 (s, C_{allyl}), 150.4 (s, C_α), 153.7 (br s, C_γ). $^{31}P\{^1H\}$ NMR (101.25 MHz, CD_2Cl_2) δ (ppm) = 18.2. IR (KBr) ν(C=N)$_{py}$ 1604 cm^{-1}. Elem. anal. for $C_{22}H_{24}ClN_2PPd$ (489.2): calcd (%) C, 54.00; H, 4.94. Found: C, 53.60; H, 4.86.

4.3.9. Synthesis of **11**

To a solution of **9** (0.030 g, 12.5 μmol) in 5 cm^3 of CH_2Cl_2, 0.054 g (0.21 mmol) of AgOTf was added, and the mixture was stirred for 2 h light protected to obtain **10**. Then, the solid was filtered through Celite and the resulted bright-orange solution was concentrated to 5 cm^3. This solution was added slowly to a solution of 0.033 g (0.05 mmol) of **4b** in 2 cm^3 of CH_2Cl_2, and stirred for 30 min. The solution was filtered and concentrated to dryness and the solid was washed with Et_2O (3 × 5 cm^3) and dried under vacuum. Compound **11** was obtained as a yellow-ochre solid in 92% yield. ^1H NMR (400.11 MHz, CD_2Cl_2) δ (ppm) = −0.64–0.04 (m, 40H, CH_3Si, CH_2Si), 0.90 (m, 24H, CH_{3cym}), 1.44 (m, 12H, CH_{3cym}), 1.90 (m, 8H, CH_2P dend), 2.46 (br s, 4H, CH_{cym}), 4.49 (br s, 8H, CH_2P), 5.00–5.68 (m, 16H, C_6H_4), 6.54 (d, 8H, $^3J_{H-H}$ = 5.1 Hz, H_β), 6.81 (br s, 4H, N*H*), 7.31–7.56 (m, 80H, C_6H_5), 7.73 (d, 8H, $^3J_{H-H}$ = 4.6 Hz, H_α). $^{13}C\{^1H\}$ NMR (62.90 MHz, CD_2Cl_2) δ (ppm) = −0.4 (s, CH_3Si^1), 2.7 (s, CH_2Si^0), 19.3 (s, CH_{3cym}), 23.8 (m, CH_{3cym}), 45.5 (br s, CH_2P), 110.2 (s, C_β), 122.7 (q, $^1J_{C-F}$ = 321.0 Hz), 129.5–135.8 (m, C_6H_5), 155.9 (s, C_α), 148.7 (br s, C_γ). $^{31}P\{^1H\}$ NMR (101.25 MHz, CD_2Cl_2) δ (ppm) = 29.6 (s, PPh_2–Au), 35.6 (s, PPh_2–Ru). $^{19}F\{^1H\}$ NMR (376.48 MHz, CD_2Cl_2) δ (ppm) = −78.9 (s, CF_3SO_3). IR (KBr) ν(C=N)$_{py}$ 1612 cm^{-1}. Elem. anal. for $C_{204}H_{212}Au_4F_{36}N_8O_{36}P_8Ru_4S_{12}Si_5$ (6001.2): calcd (%) C, 40.82; H, 3.56. Found: C, 41.38; H, 4.08.

4.3.10. Synthesis of **12**

To a solution of [4-py–*N*{CH_2–PPh_2AuCl}$_2$] (0.049 g, 0.05 mmol) in 5 cm^3 of CH_2Cl_2, 0.029 g (0.11 mmol) of AgOTf was added. The mixture was stirred 45 min at r.t. light protected. The final suspension was filtered through Celite and the solution was concentrated to 5 cm^3. Dendrimer **9** (0.030 g, 12.5 μmol) in 5 cm^3 of CH_2Cl_2 and 0.054 g (0.21 mmol) of AgOTf were added and the suspension is stirred for 2 h light protected. Then, it was filtered through Celite and the bright-orange solution was concentrated to 5 cm^3 and was slowly added to a solution of the [4-py–*N*{CH_2–PPh_2AuOTf}$_2$] complex and was stirred for 1 h. The solution was concentrated to dryness, and the solid was washed with Et_2O (3 × 2 cm^3) and dried in vacuum. Compound **12** was obtained as an orange-brown solid in 72% yield. ^1H NMR (250.13 MHz, CD_2Cl_2) δ (ppm) = −0.61–0.09 (m, 40H, CH_3Si, CH_2Si), 0.70 (d, 12H, $^3J_{H-H}$ = 6.8 Hz, CH_{3cym}), 1.01 (d, 24H, $^3J_{H-H}$ = 6.4 Hz, CH_{3cym}), 1.62–1.77 (m, 36H, CH_{3allyl}, $(CH_3)_G$, CH_2P dend, CH_{cym}), 3.14 (br s, 8H, CH_{2allyl}), 4.00 (br s, 8H, CH_{2allyl}), 4.78–5.11 (m, 16H, CH_2P), 5.64–5.94 (m, 16H, C_6H_4), 6.95–7.78 (m, 136H, H_β, C_6H_5, H_α). $^{13}C\{^1H\}$ NMR (62.90 MHz, CD_2Cl_2) δ (ppm) = −1.3 (s, CH_3Si^1), 2.6 (s, CH_2Si^0), 3.7 (s, $C^2H_2Si^0$), 10.9 (m, CH_2P_{dend}), 19.2 (s, CH_{3cym}), 22.6 (m, CH_{3cym}), 32.4 (s, CH_{cym}), 53.5 (d, ^1J(C–P) = 17.0 Hz, CH_2P), 86.7–94.3 (m, C_6H_4), 114.3 (s, C_β), 131.3–135.9 (m, C_6H_5), 152.5 (s, C_α), 155.1 (br s, C_γ). $^{31}P\{^1H\}$ NMR (101.25 MHz, CD_2Cl_2) δ (ppm) = 19.4 (s, PPh_2–Au), 25.8 (s, PPh_2–Ru). ^{19}F NMR (376.48 MHz, CD_2Cl_2) δ (ppm) = −78.8 (s, $CF_3SO_{3counterion}$), −78.3 (s, $CF_3SO_{3coordinated}$). IR (KBr) ν(C=N)$_{py}$ 1611 cm^{-1}. Elem. anal. for $C_{260}H_{256}Au_8F_{48}N_8O_{48}P_{12}Ru_4S_{16}Si_5$ (8178.3): calcd (%) C, 38.18; H, 3.15. Found: C, 39.03; H, 3.43.

4.3.11. Synthesis of **13**

To a solution of **9** (0.030 g, 12.5 μmol) in 5 cm^3 of CH_2Cl_2, 0.055 g (0.21 mmol) of AgOTf was added, and the mixture was stirred for 2 h, light protected. Then, the solid was filtered through Celite and the resulted bright-orange solution was concentrated to 5 cm^3. This solution was added slowly to a solution of 0.040 g (0.05 mmol) of **8** in 3 cm^3 of CH_2Cl_2, and was stirred for 30 min. The solution was concentrated to dryness and the solid was washed with Et_2O (3 × 5 cm^3) and dried in vacuum. The metallodendrimer **13** was obtained as a yellow solid in 93% yield. ^1H NMR (250.13 MHz, CD_2Cl_2) δ (ppm) = −0.61–0.09 (m, 40H, CH_3Si, CH_2Si), 0.70 (d, 12H, $^3J_{H-H}$ = 6.8 Hz, CH_{3cym}), 1.01 (d, 24H, $^3J_{H-H}$ = 6.4 Hz, CH_{3cym}), 1.62–1.77 (m, 36H, CH_{3allyl}, CH_{3cym}, CH_2P_{dend}, CH_{cym}), 3.14 (br s, 8H, CH_{2allyl}), 4.00 (br s, 8H, CH_{2allyl}), 4.78–5.11 (m, 16H, CH_2P), 5.64–5.94 (m, 22H, C_6H_4, H_β), 6.95–7.78 (m, 128H, C_6H_5, H_α). $^{13}C\{^1H\}$ NMR (100.61 MHz, CD_2Cl_2) δ (ppm) = −0.2 (s, CH_3Si^1), 3.0 (s, CH_2Si^0), 10.3 (s, CH_2Si^0), 11.9 (m, CH_2P_{dend}), 19.8 (s, $(CH_3)_G$), 22.7 (s, CH_{3cym}), 24.6 (s, CH_{3cym}), 25.8 (s, CH_{3allyl}), 32.6 (s, CH_{cym}), 52.6 (br s, CH_2P), 76.2 (s, CH_{2allyl}), 76.5 (s, CH_{2allyl}), 111.8 (s, C_β), 123.1 (m, $^1J_{C-F}$ = 320.9 Hz, CF_3SO_3), 130.9–135,6 (m, C_6H_5), 140.8 (s, C_{allyl}), 154.7 (s, C_α), 155.9 (br s, C_γ). $^{31}P\{^1H\}$ NMR (101.25 MHz, CD_2Cl_2) δ (ppm) = 7.2 (s, PPh_2–Pd), 29.8 (s, PPh_2–Ru). ^{19}F NMR (376.48 MHz, CD_2Cl_2) δ (ppm) = −78.9 (s, $CF_3SO_{3counterion}$), −78.4 (s, $CF_3SO_{3coordinated}$). IR (KBr) ν(C=N)$_{py}$ 1612 cm^{-1}. ESI-MS (*m*/*z*) 3164 [**10** − TfO]$^+$, 651.3 [**8** − OTf]$^+$. Elem. anal. for $C_{255}H_{284}F_{36}N_8O_{36}P_{12}Pd_4Ru_4S_{12}Si_5$ (6447.8): calcd (%) C, 47.49; H, 4.44. Found: C, 48.61; H, 5.03.

Acknowledgements

Financial support from MICINN project CTQ2009-08795 is acknowledged. P.G.S. and A.M. are supported by the Factoría de Cristalización—Consolider CSD2006-00015.

Appendix A. Supplementary material

CCDC 879273 and 879274 (for **5** and **8**) contain the supplementary crystallographic data for this paper. These data can be obtained free of charge from The Cambridge Crystallographic Data Centre *via* www.ccdc.cam.ac.uk/data_request/cif.

References

[1] F. Vögtle, G. Richardt, N. Werner, Dendrimer Chemistry: Concepts, Syntheses, Properties, Applications, Wiley-VCH, Weinheim, 2009;
A.M. Caminade, P. Servin, R. Laurent, J.P. Majoral, Chem. Soc. Rev. 37 (2008) 56–67;
A.R. Menjoge, R.M. Kannan, D.A. Tomalia, Soft Matter 6 (2010) 456–474;
M. Marcos, R. Martín-Rapún, A. Omenat, J.L. Serrano, Chem. Soc. Rev. 36 (2007) 1889–1901.

[2] D. Astruc (Ed.), Dendrimers and Nanoscience, vol. 6, C. R. Chimie, Paris, 2003;
K. Yamamoto, K. Takanashi, Polymer 49 (2008) 4033–4041;
D. Astruc, E. Boisselier, C. Ornelas, Chem. Rev. 110 (2010) 1857–1959;
D. Astruc, Tetrahedron: Asymmetry 21 (2010) 1041–1054;
A. El Kadib, N. Katir, M. Bousminaac, J.P. Majoral, New J. Chem. 36 (2012) 241–255.

[3] C.M. Casado, B. Alonso, J. Losada, Coord. Chem. Rev. 193–195 (1999) 395–445;
A.M. Caminade, R. Laurent, B. Chaudret, J.P. Majoral, Coord. Chem. Rev. 178 (1998) 793–821;
I. Cuadrado, M. Morán, S. Arévalo, E. de Jesús, F.J. de la Mata, J.C. Flores, R. Gómez, Organometallics 20 (2001) 2583–2592. and references therein;
O. Rossell, M. Seco, I. Angurell, C. R. Chim. 6 (2003) 803–817;
S.-H. Hwang, C.D. Shreiner, C.N. Moorefield, G.R. Newkome, New J. Chem. 31 (2007) 1192–1217;
D.J.M. Snelders, M.A.N. Virboul, R. Kreiter, C. Versluis, G. van Koten, R.J.M. Klein Gebbink, Dalton Trans. 41 (2012) 2354–2359;
F. Corzana, M. Monge, E. Sánchez-Forcada, Inorg. Chim. Acta 380 (2012) 31–39.

[4] A. Juris, V. Balzani, S. Campagna, G. Denti, S. Serroni, G. Frei, H.U. Guedel, Inorg. Chem. 33 (1994) 1491–1496;
G.X. Liu, R.J. Puddephatt, Organometallics 15 (1996) 5257–5259;
C.M. Casado, B. González, I. Cuadrado, B. Alonso, M. Morán, J. Losada, Angew. Chem., Int. Ed. 39 (2000) 2135–2138;
I. Angurell, G. Muller, M. Rocamora, O. Rossell, M. Seco, Dalton Trans. (2003) 1194–1200;
D. Méry, L. Plault, C. Ornelas, J. Ruiz, S. Nlate, D. Astruc, J.C. Blais, J. Rodrigues, S. Cordier, K. Kirakci, C. Perrin, Inorg. Chem. 45 (2006) 1156–1167;
M. Zamora, B. Alonso, C. Pastor, I. Cuadrado, Organometallics 26 (2007) 5153–5164;
E.J. Fernández, A. Laguna, M. Monge, M. Montiel, M.E. Olmos, J. Pérez, E. Sánchez-Forcada, Dalton Trans. (2009) 474–480.

[5] M. Benito, O. Rossell, M. Seco, G. Segalés, Organometallics 18 (1999) 5191–5193;
M. Benito, O. Rossell, M. Seco, G. Muller, J.I. Ordinas, M. Font-Bardia, X. Solans, Eur. J. Inorg. Chem. (2002) 2477–2487;
I. Angurell, J.C. Lima, L.-I. Rodríguez, L. Rodríguez, O. Rossell, M. Seco, New J. Chem. 30 (2006) 1004–1008;
L.-I. Rodríguez, O. Rossell, M. Seco, A. Grabulosa, G. Muller, M. Rocamora, Organometallics 25 (2006) 1368–1376;
L.-I. Rodríguez, O. Rossell, M. Seco, G. Muller, Organometallics 27 (2008) 1328–1333.

[6] J.A. Casares, P. Espinet, J.M. Martín-Álvarez, V. Santos, Inorg. Chem. 45 (2006) 6628–6636;
J.D.E.T. Wilton-Ely, A. Schier, N.W. Mitzel, S. Nogai, H. Schmidbaur, J. Organomet. Chem. 643–644 (2002) 313–323;
S.E. Durran, M.B. Smith, S.H. Dale, S.J. Coles, M.B. Hursthouse, M.E. Light, Inorg. Chim. Acta 359 (2006) 2980–2988.

[7] I. Angurell, O. Rossell, M. Seco, Chem.—Eur. J. 15 (2009) 2932–2940.

[8] M.A. Bennet, G.B. Robertson, A.K. Smith, J. Organomet. Chem. 43 (1972) C41–C43.

[9] S. Serron, S.P. Nolan, Y.A. Abramov, L. Brammer, J.L. Petersen, Organometallics 17 (1998) 104–110.

[10] I. Moldes, E. de la Encarnación, J. Ros, A. Alvarez-Larena, J.F. Piniella, J. Organomet. Chem. 566 (1998) 165–174.

[11] K.A. Flanagan, J.A. Sullivan, H. Müeller-Bunz, Langmuir 23 (2007) 12508–12520;
F. Thomas, T. Bauer, S. Schulz, M. Nieger, Z. Anorg. Allg. Chem. 629 (2003) 2018–2027;
Y. Takenaka, K. Osakada, Bull. Chem. Soc. Jpn. 73 (2000) 129–130.

[12] J.R. Berenguer, J. Forniés, E. Lalinde, F. Martínez, Organometallics 15 (1996) 4537–4546;
A. Scrivanti, F. Benetollo, A. Venzo, M. Bertoldini, V. Beghetto, U. Matteoli, J. Organomet. Chem. 692 (2007) 3577–3582.

[13] A. Grabulosa, G. Muller, R. Ceder, M.A. Maestro, Eur. J. Inorg. Chem. (2010) 3372–3383.

[14] I. Angurell, G. Muller, M. Rocamora, O. Rossell, M. Seco, Dalton Trans. (2004) 2450–2457.

[15] I. Angurell, O. Rossell, M. Seco, E. Ruiz, Organometallics 24 (2005) 6365–6373.

[16] D.A. White, Inorg. Synth. 13 (1972) 55–65.

[17] R. Usón, A. Laguna, Organomet. Synth. 3 (1986) 322–342.

[18] M.A. Bennett, T.N. Huang, T.W. Matheson, A.K. Smith, Inorg. Synth. 21 (1982) 74–78.

[19] L. Hirsivaara, M. Haukka, J. Pursiainen, J. Organomet. Chem. 633 (2001) 66–68;
G.R. Newkome, D.C. Hager, J. Org. Chem. 43 (1978) 947–949.

[20] J.L. Herde, J.C. Lambert, C.V. Senoff, Inorg. Synth. 15 (1974) 18–20.

[21] J. Chatt, L.M. Vallarino, L.M. Venanzi, J. Chem. Soc. (1957) 3413–3416.

[22] J.X. McDermott, J.F. White, G.M. Whitesides, J. Am. Chem. Soc. 98 (1976) 6521–6528.

[23] M. Benito, O. Rossell, M. Seco, G. Segalés, Inorg. Chim. Acta 291 (1999) 247–251.

[24] N.Y. Li, Z.G. Ren, D. Liu, R.X. Yuan, L. Wei, L. Zhang, H.X. Li, J.P. Lang, Dalton Trans. 39 (2010) 4213–4222.

[25] G.M. Sheldrick, Acta Crystallogr. A64 (2008) 112–122.

[26] R.H. Blessing, Acta Crystallogr. A51 (1995) 33–38.

[27] L.J. Farrugia, J. Appl. Crystallogr. 32 (1999) 837–838.